

Model of an oscillatory neural network with multilevel neurons for pattern recognition

Andrei Velichko*, Maksim Belyaev and Petr Boriskov

Institute of Physics and Technology, Petrozavodsk State University, 31 Lenina str., Petrozavodsk 185910, Russia

* Corresponding author: e-mail velichko@petrsu.ru

Abstract

The article presents a study on a new type of an oscillatory neural network (ONN) that uses multilevel neurons for pattern recognition on the basis of high order synchronization effect. The feature of this network architecture is a single oscillator (neuron) at the output with multilevel variation of its synchronization value with the main oscillator thus allowing classifications of an input pattern into a set of classes. ONN model is realized on thermally-coupled VO_2 -oscillators. ONN training was performed by using the trial-and-error method for the network parameters selection. It is shown that ONN is capable to classify 512 visual patterns (as a cell array 3x3, distributed by symmetry into 102 classes) into a set of classes with the maximum number of elements up to $P=11$. Classification capability of a network is studied depending on the interior noise level and synchronization effectiveness parameter. The obtained results allow designing multilevel output cascades of neural networks with high net data throughput and it may be applied in ONNs with various coupling mechanisms and oscillators topology.

Keywords: oscillatory neural networks, pattern recognition, higher order synchronization, thermal coupling, vanadium dioxide.

1. Introduction

Hypotheses of functional importance of synchronization for information processed by the brain were put forward long ago [1], [2] and its experimental discovery [3], [4] encouraged creation of neural networks models with oscillatory dynamics and of neuromorphic algorithms of image processing based on synchronization [5]–[7].

Research of oscillatory neural networks is mainly based of the models of phase oscillators with slow variation in oscillation amplitude in a narrowband spectrum. Such models, primarily Kuramoto model [8], appeared to be very useful for studying systems of various topology with a large number ($N>10^3$) of oscillators, where such modes as global and cluster synchronization, synchronization by middle field [9] and mode of quasisynchronization [10] are feasible.

Alternatively, there is another class of ONN based on relaxation oscillators that generate multiple pulses of short duration and fixed amplitude. Such pulses (spikes) can code information at pulse-repetition frequency. There is an important distinguishing feature of a pulse type ONN from classic spiking neural networks (SNN): it is a self-oscillating mode of ONN neuro-oscillators, that is not indicative for either SNN, or real (biological) neurons performance because they are

characterized by a forced response through generation of a single spike or their group when the neuron threshold level is achieved. However, ONNs are fascinating due to simplicity of hardware implementation and because the developed micro- and nanoelectronic self-oscillators can ensure their compactability and energy efficiency.

Also pulse type ONNs with multifrequent periodic oscillation spectrum feature a specific mode of multiple frequency synchronization or, in other words, high order synchronization effect [11]. We have recently demonstrated this effect experimentally by the example of thermally-coupled VO₂-oscillators [12]. In relaxation oscillators with vanadium dioxide-based film elements electric self-oscillations are activated by the effect of electric switching governed by metal – insulator transition (MIT) [13]–[16]. Such features as processing speed of switching VO₂ devices amounting to (~10 ns) [17] and manufacturing technology that allows switching elements to be created with high level of nanoscalability make VO₂-switch based oscillators perfect objects for research on neuro-oscillators ensembles to solve cognitive technology problems [18]–[21].

It should be noted that relaxation oscillators with high order synchronization effect can be realized by using electric coupling [18]–[21] and also by using not only VO₂-switches but any other switching elements such as thyristors [22], tunneling diodes [23], resistive memory cells [24], spin torque oscillator [25], etc.

In the present paper, we study ONN of thermally-coupled VO₂-oscillators and present a general concept of visual patterns recognition based on high order synchronization effect. We use the property of this effect – multiplicity of synchronous states variants – to extract object classes by using a single output oscillator and to realize uniquely high network throughput rate.

2 Method

2.1 Oscillator circuit and method of ONN organization

The basic element in the studied ONN is an oscillator implemented on the circuit of a relaxation generator (Fig. 1a) based on a VO₂-switch. We described in detail in [12] the process of fabrication and electric I-V characteristics of an electric VO₂-switch. I-V characteristic is approximated well by a piecewise linear function that has two conduction states (low-resistance and high-resistance) and also a region of negative differential resistance (NDR). These switches may be used in the circuit of a relaxation generator with power supply I_p holding the operation point in the region NDR of I-V characteristic and with capacity C, parallel connected to the switch. In addition, there is a source of noise U_n that models circuit interior or exterior noises, for instance, current noise of a switch [26]. Oscillator output signal is current $I_{sw}(t)$ flowing through VO₂-switch that is used to calculate synchronization level of two oscillators (see section 2.3). Besides, current signal directly conditions the effect of thermal coupling inside the network.

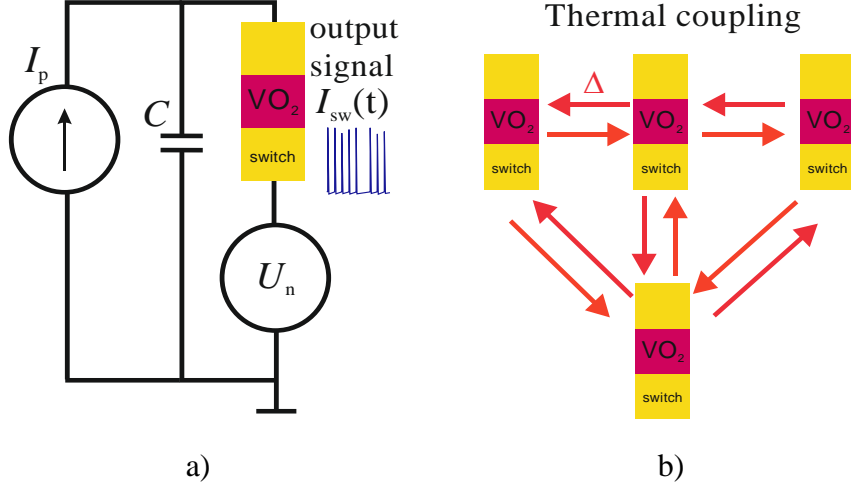


Fig. 1. Oscillator circuit (a) and example of oscillators' interaction via thermal coupling of VO_2 switches (b). $I_{sw}(t)$ – current signal in a VO_2 switch which is an output signal; U_n – source of noise.

We used thermal coupling to connect oscillators in a network [12], [27]. Thermal coupling mechanism is based on mutual thermal effect of switches due to their Joule heating and dependence of gate threshold voltage U_{th} on temperature. The choice of this coupling type is determined by the simplicity of a computing model realization when oscillators are electrically separated from each other unlike in capacitive or resistive couplings [14], [15], [18], [21]. An example of oscillators' interaction organization via thermal coupling of VO_2 switches is shown in Fig. 1b. The model of thermal coupling is based on reduction of gate threshold voltage U_{th} by the value Δ at thermal effect of other switches. This effect, as we have already said, is determined by Joule heat generation on switches when pulse current is flowing through them at the moment of capacity discharge C . More detailed presentation of the mathematical model of thermally coupled relaxation oscillators is given in our previous paper [28].

It should be noted that we also use the concept of one-way thermal coupling of oscillators in the numerical model, it may be realized physically when a resistance heater is used as a connecting element in one of the circuits instead of a switch [27].

For numerical modeling we used the following parameters of I-V characteristic ($U_{th} = 5$ V, $U_h = 1.5$ V, $U_{bv} = 0.82$ V, $R_{off} = 9.1$ k Ω , $R_{on} = 615$ Ω). In this circuit capacity is a constant parameter $C = 100$ nF, its value significantly determines the frequency range of oscillator operation [29], and its natural frequency F_0 . In our case frequency range was 165 Hz $\leq F_0 \leq 1266$ Hz at the range of feeding currents 550 μ A $\leq I_p \leq 1061$ μ A.

2.2 ONN structure

The studied ONN consists of an input pattern that translates a pattern as 3×3 matrix on the layer of processing neurons including 10 oscillators, and of an output layer with only one oscillator (output neuron) №11 (see Fig. 2). The layer of processing neurons consists in its turn of a 3×3 oscillator matrix connected by similar couplings ($\Delta_{i,j}=\Delta_{j,i}=\Delta_{\text{mat}}$, where i, j are the numbers of neighbor oscillators), connection between neighbor oscillators is made only by horizontal and vertical lines. Thus, the central oscillator №6 has four couplings in the matrix, the corner oscillators have two couplings, and the oscillators in the center of faces have three couplings (with the central oscillator and two corner ones). Besides, there is the basic oscillator №1 (first neuron) on the processing layer and the synchronization order of all other oscillators is measured against this oscillator. Oscillator №1 (Fig. 2) affects unidirectionally all other oscillators in this matrix ($\Delta_{1,i}\neq 0=\Delta_1$, и $\Delta_{i,1}=0$, где $i=2\dots 10$) and they in their turn affect unidirectionally oscillator №11 (output neuron) in the output layer ($\Delta_{i,11}\neq 0=\Delta_{11}$ и $\Delta_{11,i}=0$, where $i=2\dots 10$).

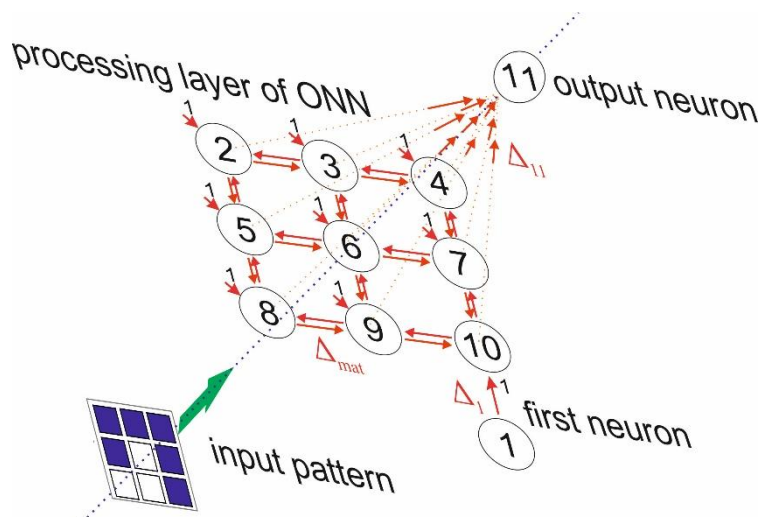


Fig. 2. ONN organization circuit for pattern recognition as a matrix of 3×3 elements. Digits indicate the sequence numbers of oscillators.

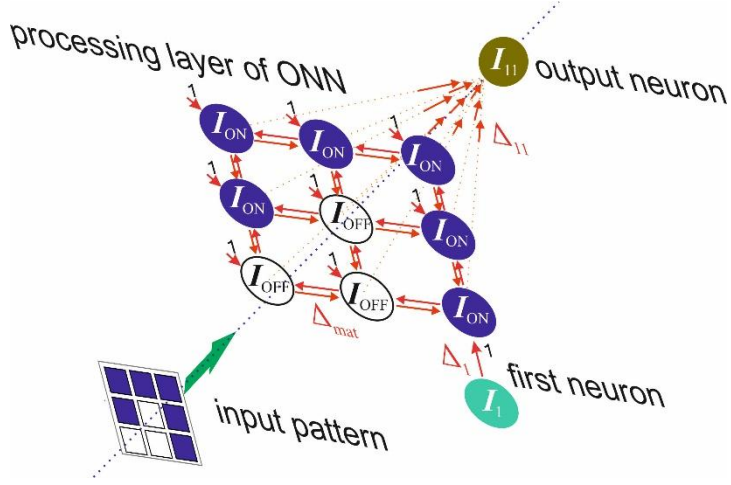


Fig. 3. Principle of a pattern translation from the input layer to the oscillator matrix via setting of their currents (I_{OFF} is for white squares, I_{ON} is for blue squares). Separate colors are used for oscillators №1 and №11 and for their currents I_1 and I_{11} , respectively.

Pattern translation (see Fig. 3) on the processing layer is performed by selection of feeding currents of oscillator matrix taking values $I_{p,i} = I_{ON}$ or $I_{p,i} = I_{OFF}$ (where $i=2\dots10$), that corresponds to white (I_{OFF}) and blue (I_{ON}) colors of input pattern squares. Pattern translation in the intermediate layer causes change in oscillators feeding currents that in its turn leads to change of synchronization state for all oscillators (№2 - 11). In this case the synchronization order $SHR_{1,11}$ between the basic oscillator №1 and the oscillator in the output layer №11 serves as the control value. The values of feeding currents for these oscillators are fixed and may differ from currents in the matrix, therefore they are indicated as I_1 and I_{11} (see. Fig.3).

2.3 Method of synchronization order definition

To denote high-order synchronization value for N interacting oscillators in [30] we worked out the ratio of integers $k_1:k_2:k_3:\dots:k_N$, where k_N is harmonic order of N -th oscillator at the common frequency of the network synchronization F_s . In our case when we define synchronization order only between two oscillators (№1 и №2-11), it is possible to use the concept of subharmonics ratio as in [12], that is defined as a simple fraction $SHR_{i,j}=k_i:k_j \sim k_i/k_j$, where i and j are the oscillators numbers between which the synchronization order is measured. It is obvious that to define the synchronization order for the first oscillator $SHR_{1,1}$ in relation to itself is not reasonable because $SHR_{1,1}=1$.

In our study the main technical problem was the problem of defining the synchronization order between the first (basic) oscillator №1 and the oscillator of the output layer №11 characterized by the value $\text{SHR}_{1,11}$:

$$\text{SHR}_{1,11} = k_1 : k_{11} \sim k_1 / k_{11} . \quad (1)$$

It can be seen that the same value of $\text{SHR}_{1,11}$ may be expressed in several ways: as a ratio, a simple fraction or a real number, for example, $\text{SHR}_{1,11}=10:3=10/3=3.33$. Further, we will use this property to present the results more vividly.

The method of SHR definition for two oscillators is described in detail in our papers [12]. The presence or absence of synchronization was determined by a threshold method by using the value of synchronization effectiveness η so that at $\eta \geq \eta_{\text{th}}$ the two-oscillator system was considered as being synchronized. We varied the threshold value η_{th} during the numerical experiment. Nevertheless, the commonly used value is $\eta_{\text{th}}=90\%$ in most cases (where it is not specified).

Current oscillograms $I_{\text{sw}}(t)$ of oscillators №1-11 were calculated simultaneously and contained $\sim 250\ 000$ points with time interval $\delta t=10\mu\text{s}$. After that the oscillograms were automatically processed, synchronization order $\text{SHR}_{1,i}$ was determined, where $i=2\dots 11$.

The switch parameters did not change in numerical simulation of the results (see section 2.1), but current intensities $I_{\text{p_i}}$ ($I_{\text{ON}}, I_{\text{OFF}}, I_1, I_{11}$), coupling strength constants Δ ($\Delta_1, \Delta_{11}, \Delta_{\text{mat}}$), noise amplitude U_n and η_{th} varied.

2.4 Pattern classifier implementation and problems definition

A “black-and white” pattern is used as an input test pattern presented as a 3×3 matrix (without gradation of gray color, 3 by 3 pixels) where each cell may take the value 0 (white color) or 1 (blue color). The total number of patterns (figures) in the input layer matrix is $2^9=512$. Presuming that the pattern processing layer together with the output layer has certain symmetry, a set of 512 figures may be divided into 102 classes (see Fig. 4).

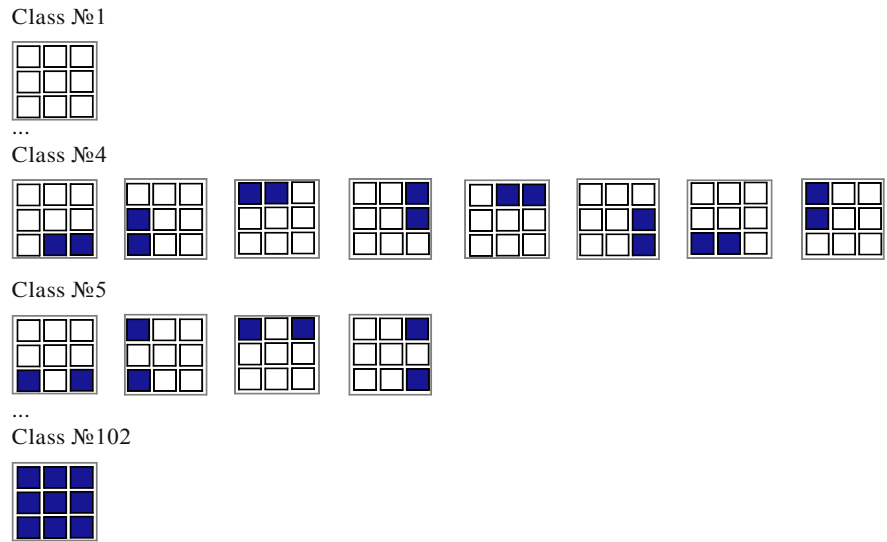


Fig. 4. Symmetry-based distribution of 512 figures into 102 classes.

The principle of figures distribution into classes is the following: in each class the figures have the same number of blue (white) cells and rotation-reflection axial symmetry of the 4th order (symmetry at rotation by 90°).

Mirror -rotation axial symmetry of the 4th order presupposes association of all figures in a separate class in the mirror operation in relation to the central columns (horizontally and vertically) and also at rotation by 90° (see the example of transformation for class №4 figures in Fig. 5).

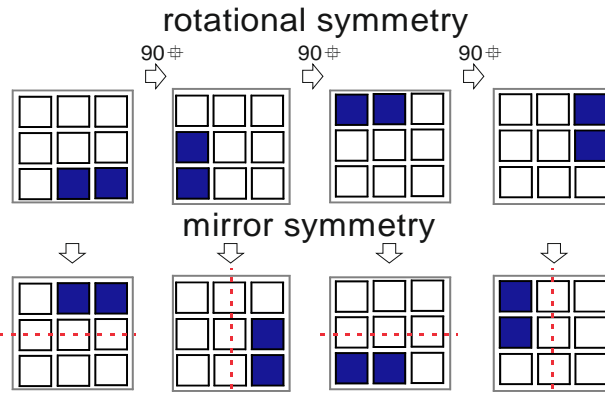


Fig. 5. Mirror -rotation axial symmetry of the 4th order in class №4.

Figures from one class impose absolutely the same effect on the neural network and, respectively, have the same output value $SHR_{1,11}$. Thus, distribution into classes allows us to find figures that at any values I_{p_i} (I_{ON} , I_{OFF} , I_1 , I_{11}) and also Δ (Δ_1 , Δ_{11} , Δ_{mat}), noise amplitude U_n and η_{th} , will have the same values of synchronization effectiveness η and $SHR_{1,11}$ within one class of figures as a result of neural network symmetry.

On the other hand, such initial distribution of all 512 figures into classes allows us to recognize not one specific figure but a class (out of 102 possible ones) into which this figure is classified. Besides, such classification reduces the number of possible variants of figures numerical sorting in analysis of neuron network operation as we may send only 102 figures to the input layer, one figure per each class.

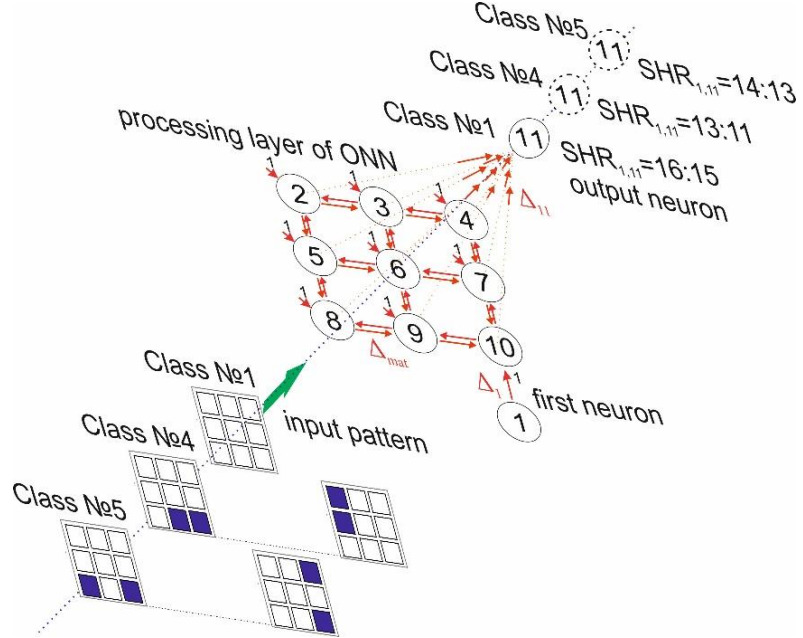


Fig. 6. Principle of class recognition of neural network figures with one output neuron.

The problems that this neural network is able to solve may be divided into several variants:

- I. Synchronization of oscillators №1 и №11 with the corresponding value of $SHR_{1,11}$, exists only for one specific class with number (Class № S) out of 102 possible variants. The problem may be expressed by the formula:

$$SHR_{1,11} = \begin{cases} k_1 \cdot k_{11} \text{ and } \eta \geq \eta_{th} \text{ if Class } N_c = \text{Class } N_S \\ \text{no synchronisation and } \eta < \eta_{th} \text{ if Class } N_c \neq \text{Class } N_S \end{cases}, \quad (2)$$

where the class number N_c changes within all possible range $N_c=1...102$.

- II. There is a set of classes S with the elements number P ($P < 102$), $S = \{\text{Class } N_1, \text{Class } N_2, \dots, \text{Class } N_P\}$, for which there is a corresponding set of high order synchronizations $SHR = \{SHR^{(1)}_{1,11}, SHR^{(2)}_{1,11}, \dots, SHR^{(P)}_{1,11}\}$ with the same number of elements. The set SHR does not have the same elements, i.e. each class of figures from set S corresponds to a unique synchronization order $SHR_{1,11}$. By analogy with (2) the problem may be expressed as:

$$\text{SHR}_{1,11} = \begin{cases} \text{SHR}_{1,11}^{(1)} \text{ and } \eta \geq \eta_{\text{th}} \text{ if Class } \text{№ } N_c = \text{Class } \text{№ } S_1, \\ \text{SHR}_{1,11}^{(2)} \text{ and } \eta \geq \eta_{\text{th}} \text{ if Class } \text{№ } N_c = \text{Class } \text{№ } S_2, \\ \dots, \\ \text{SHR}_{1,11}^{(P)} \text{ and } \eta \geq \eta_{\text{th}} \text{ if Class } \text{№ } N_c = \text{Class } \text{№ } S_p, \\ \text{no synchronisation and } \eta < \eta_{\text{th}} \text{ if Class } \text{№ } N_c \notin S \end{cases}, \quad (3)$$

Where the class number N_c changes within all possible range $N_c=1\dots102$. Actually problem I is a subcase of problem II at $P=1$.

The principle of realization for problem II solution is shown in Fig. 6. Here $P=3$, and set $S=\{\text{Class } \text{№ } 1, \text{Class } \text{№ } 4, \text{Class } \text{№ } 5\}$, in this case the corresponding set is $\text{SHR}=\{16:15, 13:11, 14:13\}$. Thus, unambiguous recognition of figures belonging to three different classes occurs. Synchronization is not realized for all other classes and $\eta < \eta_{\text{th}}$.

III. The third variant of the problem may be ideal network learning to solve problem II at $P=102$. In this problem each class out of 102 possible variants corresponds to its unique value of synchronization order $\text{SHR}_{1,11}$.

Actually, problems I-III have increasing degree of complexity and are subcases of problem II with different parameter P . Nevertheless, it should be noted that problem I is the simplest one which may be solved by a common neural network with one bistable output neuron (bistability means presence or absence of synchronization), although two variants of answers in neural networks are more often organized by using two output neurons [31].

Whereas the output neuron in problems II and III should have multilevel properties, thus being different from a common bistable neuron. All three problems may be set for the circuit shown in Fig. 2. We should note the most striking difference of this neural network from variants presented in the literature. The ONN circuit has only one output neuron, nevertheless, the effect of multilevel high order synchronization used here and characterized by value $\text{SHR}_{1,11}$ allows input pattern classification into P classes within set S . This increases net data throughput of a single neuron and enables us to create multilevel output cascades of neural networks with high functionality.

2.5 Technique of ONN training

To solve problems I-III it is necessary to be able to train the network. As the ONN with the high order synchronization effect has not been studied before there are no specially developed methods of this network training. One of the obvious ways here is to use the trial-and-error method for the network parameters selection: currents ($I_{\text{ON}}, I_{\text{OFF}}, I_1, I_{11}$), couplings strength ($\Delta_1, \Delta_{11}, \Delta_{\text{mat}}$), noise amplitude U_n and synchronization effectiveness threshold η_{th} .

To realize direct searching of all parameters we should first determine the ranges and steps (number of grades) of their variations. In our numerical experiment current range was determined by the presence of a single oscillator generation effect. So, for the oscillator circuit described in section 2.1 the generation was within the feeding current range of $550 \mu\text{A} \leq I_p \leq 1061 \mu\text{A}$. Therefore, the currents (I_{ON} , I_{OFF} , I_1 , I_{11}) also varied in this range. We determined the variation steps as $\delta I_p = 1 \mu\text{A}$. So there were only 512 current grades.

For coupling strength Δ variation range was determined by the threshold values of I-V characteristic of a switch. So the condition when integral thermal action on the neuron Δ_{Σ} should not reduce the threshold voltage of I-V characteristic of a switch U_{th} below the holding voltage must be met:

$$U_{\text{th}} - \Delta_{\Sigma} > U_h. \quad (4)$$

On the basis of formula (4), values of threshold voltages ($U_{\text{th}}=5 \text{ V}$, $U_h=1.5 \text{ V}$) and couplings configurations (see Fig. 2) the limits of coupling strength variation are subject to the following conditions: $0 \leq \Delta_1 < (3.5-4 \cdot \Delta_{\text{mat}})$, $0 \leq \Delta_{11} < (3.5/9)$, $0 \leq \Delta_{\text{mat}} < ((3.5/4)-\Delta_1)$, where units for values Δ are volts. The spacing was chosen as $\delta\Delta = 0.1 \text{ V}$.

Range $20 \mu\text{V} \leq U_n \leq 900 \mu\text{V}$ with the number of grades equal 12 was chosen for the noise amplitude.

For the synchronization effectiveness threshold η_{th} the variation range was $15 \% \leq \eta_{\text{th}} < 100\%$, with the number of grades equal 25 and minimal spacing $\delta\eta_{\text{th}}=1\%$. Here we should specify that η_{th} does not belong to the network parameters but rather to the parameters of the algorithm of synchronization order $\text{SHR}_{1,11}$ calculation. Nevertheless, the value η_{th} strongly affects the result of synchronization definition and the results of pattern recognition as a whole, because it is a conditionally chosen characteristic. Identifying its optimal value for the recognition problems solution is an important step in a network tuning and training.

There are a lot of network parameters and each parameter variant should be calculated in 102 classes together with oscillograms and synchronizations values $\text{SHR}_{1,11}$ calculations at each stage; it is obvious that full direct searching of all parameters variants will take a lot of time and computational resources.

Therefore, we developed software that enabled direct search of only one specific parameter, in particular, one of the currents (I_{ON} , I_{OFF} , I_1 , I_{11}), in this case all other parameters were fixed and selected on the basis of our experience of working with the model.

For the pattern recognition experiments we used a workstation (Intel Xeon quad core processor, 4x2 GHz, 8GB RAM) running 64 bit Windows Server 2008. CPU time cost by a single run on a one core for the direct search procedure of all 512 current grades took ~ 2.4 hours.

In conclusion, for this section we should note that direct search is not an effective training method and development of more efficient algorithms for this type of networks is a separate global problem for future research.

3. Results

As we have mentioned before, to solve problems I-III we should be able to train the network, and one of the obvious variants is direct search of parameters values (I_{ON} , I_{OFF} , I_1 , I_{11}), (Δ_1 , Δ_{11} , Δ_{mat}), U_n and η_{th} .

Solution of problem I.

We have fixed the values of the following parameters ($I_{OFF}=918\mu A$, $I_1=750\mu A$, $I_{11}=750\mu A$), ($\Delta_1=0.2$ B, $\Delta_{11}=0.1$ B, $\Delta_{mat}=0.1$ B), ($U_n=200\mu V$, $\eta_{th}=90\%$) and varied the value I_{ON} as described in section 2.5. It appeared that solution of problem I is easily found for some classes. For example, at $I_{ON}=797\mu A$ (see Fig.7a) we have a neural network that recognizes Class №102 with the corresponding synchronization order $SHR_{1,11}=10:9$, in this case there is no synchronization for all other classes.

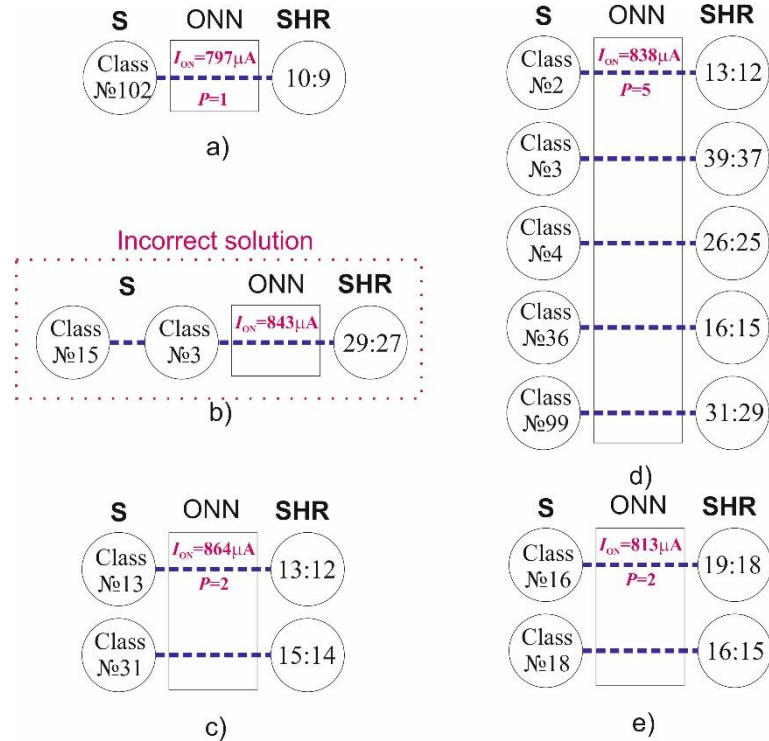


Fig. 7. Training results at various values of current I_{ON} : examples of correct (a) and incorrect (b) solutions of problem I; examples of correct solutions of problem II (c)-(e).

It should be noted that incorrect solution of training, which do not correspond to the problem I conditions occur rather often, for example, when two or more classes correspond to the

same value of $\text{SHR}_{1,11}$ (see Fig.7b). Such neural network parameters result in ambiguous recognition of figures and their classes. The same holds true for frequent cases of wrong training when there is no oscillatory synchronization for any input class (figure).

Solution of problem II.

If to analyze all results of direct search of current values I_{ON} , which arose in problem I solution with the same network parameters, then we will see that there will be solution variants for problem II as well. Fig. 7 demonstrates the variant of set **S** and **SHR** for $P=2$, and Fig. 7d demonstrates the variant of set **S** and **SHR** for $P=5$.

The condition of problem II requires that a certain class from set **S** should correspond to the unique synchronization order from set **SHR**, at the same time there is no output oscillator synchronization for other classes.

Table 1 presents a list of found current values I_{ON} , when the conditions for problem II are met for all emerging values P . It can be seen that value P reaches its maximum $P=7$. Naturally, there might be more than one solution with $P \geq 1$. For example, solution with $P=2$ is obtained both at currents $I_{\text{ON}} = 864\mu\text{A}$ and $I_{\text{ON}} = 813\mu\text{A}$, see Fig. 7c, e, and also at some other current values. Therefore, we have introduced quantity N_P that is equal to the total number of solutions for the given value P during direct search of I_{ON} . Values of N_P are also given in Table 1. It can be seen from the table that the most frequent solution appears for $P=1$ ($N_P=19$) and the number of solutions reduces with the increase of P .

Table 1. Variants of current values I_{ON} , at which problems I – II are solved for various P and the corresponding number of their solutions N_P .

| P | $I_{\text{ON}}(\mu\text{A})$ | N_P |
|-----|--|-------|
| 1 | 762, 797, 803, 849, 865, 934, 950, 954, 962, 977, 982, 992, 1001, 1010, 1020, 1031, 1038, 1042, 1051 | 19 |
| 2 | 813, 814, 816, 834, 864, 867, 952, 1061 | 8 |
| 3 | 638, 789, 806, 825, 833, 842, 866, 1052 | 8 |
| 4 | 828, 1034, 1035 | 3 |
| 5 | 838 | 1 |
| 6 | 790 | 1 |
| 7 | 792 | 1 |

Figure 8 demonstrates statistics of values $\text{SHR}_{1,11}$ variation for various values P , here the synchronization order is given as a real number (see section 2.3). In other words, this figure shows all possible values $\text{SHR}_{1,11}$ for all values I_{ON} from Table 1.

It can be seen that $\text{SHR}_{1,11}$ has an average value ~ 1.079 , in this case the range of variation is small with maximum deviation from the average value ~ 0.103 . We suppose that weak dependence of $\text{SHR}_{1,11}$ on currents I_{ON} and I_{OFF} is conditioned by the permanence of currents $I_1=750\mu\text{A}$, and $I_{11}=750\mu\text{A}$ that determine natural frequencies of outermost oscillators, and in this particular case the currents are equal. Equality of natural frequencies of oscillators №1 and №11 sets the variation area of $\text{SHR}_{1,11}$ near $\text{SHR}_{1,11}=1:1=1$. Thus, the matrix of processing layer oscillators just deviates the value $\text{SHR}_{1,11}$ from some average one.

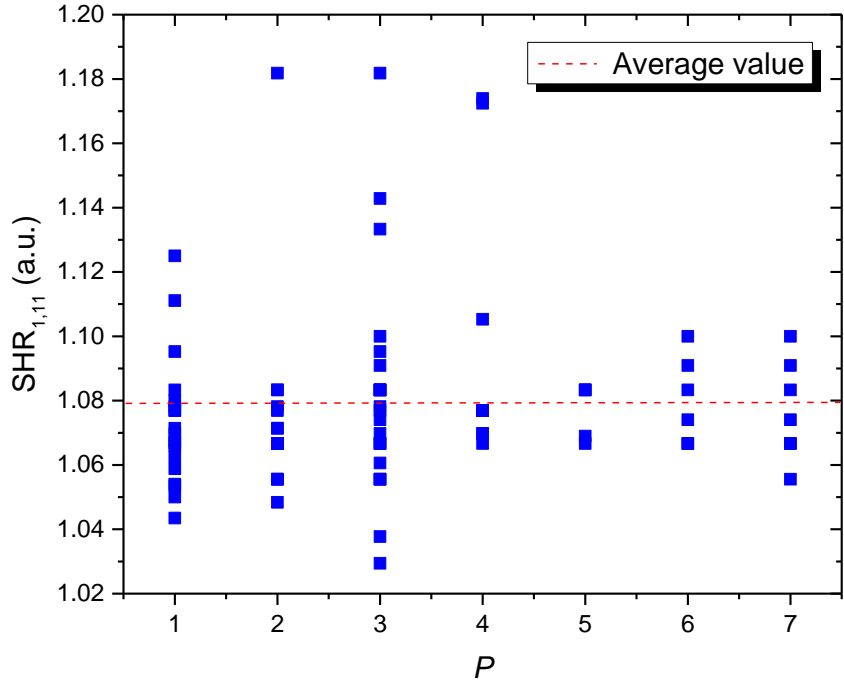


Fig. 8. Values $\text{SHR}_{1,11}$ at various P for all variants I_{ON} from Table 1. Dashed line indicates the level of average value.

We constructed a 3D graph shown in Fig.9 to find the dependence of maximum possible P and N_p on the noise amplitude value in network U_n .

It can be seen that when the noise increases above $U_n = 400 \mu\text{V}$ the number of solutions N_p and the value P sharply fall down. In this case the maximum value of P still does not exceed $P = 7$ and occurs in a wide noise range up to $U_n \leq 200 \mu\text{V}$. The basic quantity of solution variants is distributed in the range $1 \leq P \leq 4$. It is interesting that the maximum value for N_p corresponds to $P = 2$ at noise level $U_n = 100 \mu\text{V}$. In this case the integral value $\sum N_p$ for all values P also has

maximum for $U_n=100 \mu V$. Therefore, we may speak about the presence of stochastic resonance when a certain level of noise induces maximum number of solutions for problem II. The latter might be caused by two differently directed tendencies of N_p reduction: occurrence of “extra” synchronizations with decreasing U_n and suppression of synchronization number with increasing U_n .

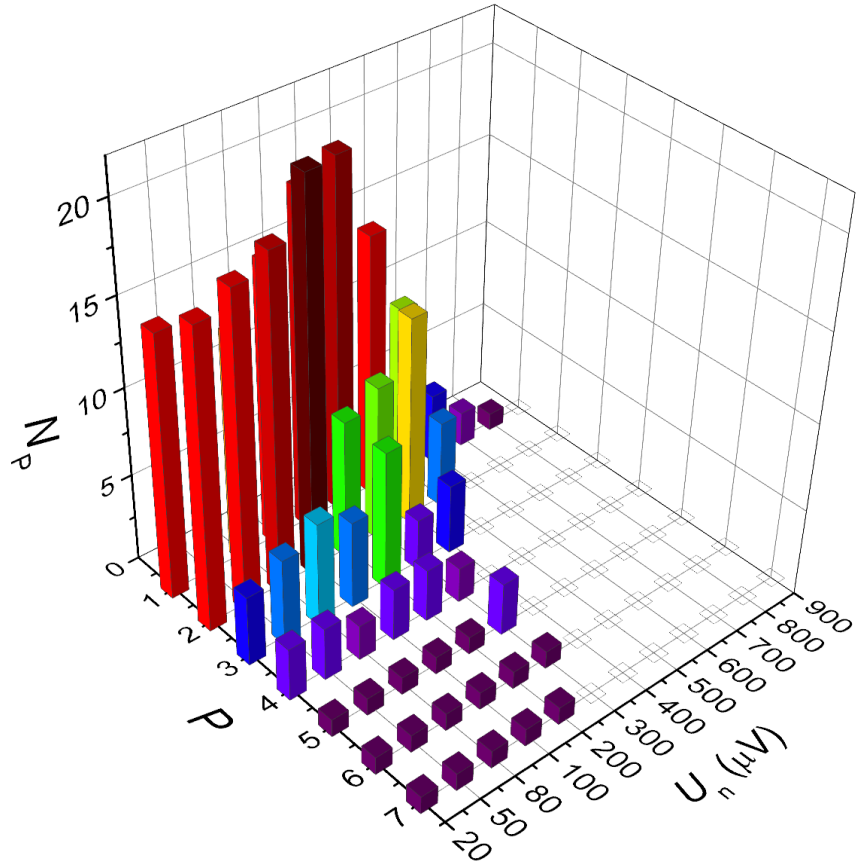


Fig. 9. Dependence of solution number N_p for various values of P on noise level U_n .

We constructed a 3D graph shown in Fig.10 to find the dependence of maximum possible P and N_p on the value of threshold synchronization effectiveness.

A general tendency for reduction of N_p at reduction of η_{th} below 40% can be seen, in this case it is interesting to note that growth of η_{th} up to $\eta_{th}=99\%$ in average does not change the values of P and N_p . This seems to be caused by the fact that synchronization occurring during problems I and II solution has a high value of effectiveness $\eta>99\%$. In this case reduction of η just adds “extra” synchronous states which do not meet the problems conditions.

The presence of maximum possible P reaching $P = 11$ at $\eta_{th} = 35\%$ is also an interesting fact. In this case we can also observe some resonance for values of P . Its presence might be caused

by reduction of maximum P both at growth of η_{th} , conditioned by solutions discarding and at reduction of η_{th} conditioned by emerging of “extra” synchronizations.

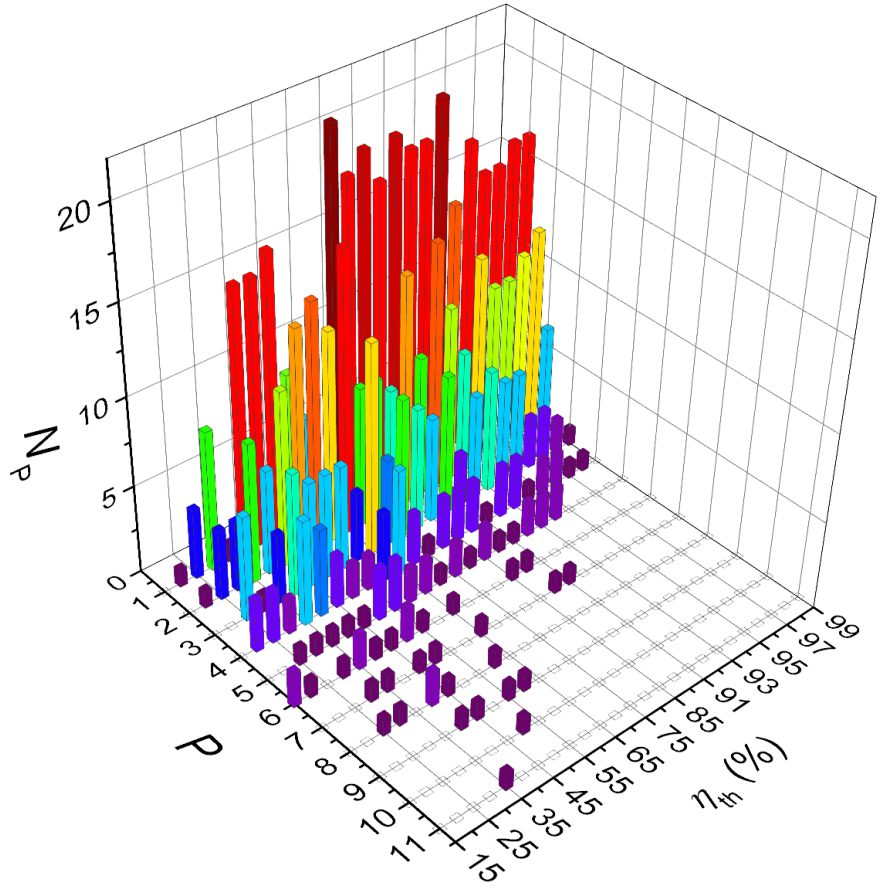


Fig. 10. Dependence of solution number for various values of P on the threshold synchronization effectiveness η_{th} .

Solution of problem III

Solution of problem III when ideal training is realized and each class out of 102 possible ones corresponds to its own unique value of synchronization order $\text{SHR}_{1,11}$ has not been found yet (see section 4).

4. Discussion and Conclusion

This paper presents a new model of ONN with high order harmonics synchronization that classifies (recognizes) two-dimensional visual patterns by unique synchronous states, i.e. in accordance with their definite symmetry class. The most outstanding feature of this neural network in comparison with variants published is that neurons possess not only bistable properties (presence or absence of synchronization with the basic neuron) but have multilevel synchronization. The mode considered here has only one output neuron, nevertheless, variation of the value of high order synchronization $\text{SHR}_{1,11}$ allows its usage to classify the input pattern into P classes with the set \mathbf{S} .

Actually parameter $SHR_{1,11}$ belongs to the properties of an output neuron while the first (basic) neuron may be considered as a master generator in regard to which we calculate synchronization of other network neurons.

Multilevel high order synchronization increases net data throughput of a single neuron and enables creating multilevel output cascades of neural networks with high functionality.

It is shown that the problem of a network training may be solved by direct search of the values of oscillators' feeding currents for the variant of incomplete classification when the number of patterns is less than the maximum number of classes ($P < 102$). We have found solution for problem II with the maximum value $P = 11$.

Solution of the problem of complete classification (problem III) when ideal training is realized and each class out of 102 possible ones corresponds to its own unique value of synchronization order $SHR_{1,11}$ has not been found yet. The ways of its solution are related to more expanded direct search of possible ONN parameters. For example, we may vary the parameters of I-V characteristic, the configuration of the network, distribution of coupling strength or the method of pattern translation into a network. Besides, an additional argument for searching new and more effective methods of pattern translation into ONN is that $SHR_{1,11}$ varies only in a very narrow range near the average value (see Fig. 8). Addition of alternative methods of pattern translation into a network that vary, for example, current I_{11} may significantly expand the range of variations and thus the maximal attainable value P .

Besides, the technique of SHR determination may affect the result and future research aimed at its improvement also may lead to positive shift in this field.

In conclusion, we should note again that development of ONN models with high order synchronization effect hold the significant potential for increasing informational capacity and efficiency of artificial intelligence networks and development of their training techniques is an important direction for further research.

Acknowledgments

This research was supported by Russian Science Foundation (grant no. 16-19-00135).

The authors express their gratitude to Dr. Dobrynina for some valuable comments in the course of the article translation.

References

[1] W. J. Freeman, "Spatial properties of an EEG event in the olfactory bulb and cortex," *Electroencephalogr. Clin. Neurophysiol.*, vol. 44, no. 5, pp. 586–605, May 1978.

- [2] C. von der Malsburg, “The Correlation Theory of Brain Function,” Springer, New York, NY, 1994, pp. 95–119.
- [3] C. M. Gray and W. Singer, “Stimulus-specific neuronal oscillations in orientation columns of cat visual cortex.,” *Proc. Natl. Acad. Sci. U. S. A.*, vol. 86, no. 5, pp. 1698–702, Mar. 1989.
- [4] R. Eckhorn *et al.*, “Coherent oscillations: A mechanism of feature linking in the visual cortex?,” *Biol. Cybern.*, vol. 60, no. 2, pp. 121–130, Dec. 1988.
- [5] M. Kuzmina, E. Manykin, and I. Surina, “Oscillatory network with self-organized dynamical connections for synchronization-based image segmentation,” *Biosystems*, vol. 76, no. 1–3, pp. 43–53, Aug. 2004.
- [6] F. CORINTO, M. BONNIN, and M. GILLI, “WEAKLY CONNECTED OSCILLATORY NETWORK MODELS FOR ASSOCIATIVE AND DYNAMIC MEMORIES,” *Int. J. Bifurc. Chaos*, vol. 17, no. 12, pp. 4365–4379, Dec. 2007.
- [7] D. E. Nikonorov *et al.*, “Coupled-Oscillator Associative Memory Array Operation for Pattern Recognition,” *IEEE J. Explor. Solid-State Comput. Devices Circuits*, vol. 1, pp. 85–93, Dec. 2015.
- [8] J. A. Acebrón, L. L. Bonilla, C. J. Pérez Vicente, F. Ritort, and R. Spigler, “The Kuramoto model: A simple paradigm for synchronization phenomena,” *Rev. Mod. Phys.*, vol. 77, no. 1, pp. 137–185, Apr. 2005.
- [9] V. V Klinshov and V. I. Nekorkin, “Synchronization of delay-coupled oscillator networks,” *Physics-Uspekhi*, vol. 56, no. 12, pp. 1217–1229, Dec. 2013.
- [10] E. Vassilieva, G. Pinto, J. Acacio de Barros, and P. Suppes, “Learning Pattern Recognition Through Quasi-Synchronization of Phase Oscillators,” *IEEE Trans. Neural Networks*, vol. 22, no. 1, pp. 84–95, Jan. 2011.
- [11] A. Pikovsky, M. Rosenblum, and J. (Jürgen) Kurths, *Synchronization : a universal concept in nonlinear sciences*. Cambridge: Cambridge University Press, 2001.
- [12] A. Velichko, M. Belyaev, V. Putrolaynen, V. Perminov, and A. Pergament, “Thermal coupling and effect of subharmonic synchronization in a system of two VO₂ based oscillators,” *Solid. State. Electron.*, vol. 141, pp. 40–49, Mar. 2018.
- [13] J. Sakai, “High-efficiency voltage oscillation in VO₂ planer-type junctions with infinite negative differential resistance,” *J. Appl. Phys.*, vol. 103, no. 10, p. 103708, May 2008.
- [14] N. Shukla *et al.*, “Synchronized charge oscillations in correlated electron systems,” *Sci. Rep.*, vol. 4, no. 1, p. 4964, May 2015.
- [15] P. Maffezzoni, L. Daniel, N. Shukla, S. Datta, and A. Raychowdhury, “Modeling and Simulation of Vanadium Dioxide Relaxation Oscillators,” *IEEE Trans. Circuits Syst. I Regul. Pap.*, vol. 62, no. 9, pp. 2207–2215, Sep. 2015.
- [16] M. A. Belyaev *et al.*, “Switching Channel Development Dynamics in Planar Structures on the Basis of Vanadium Dioxide,” *Phys. Solid State*, vol. 60, no. 3, pp. 447–456, Mar. 2018.
- [17] P. P. Boriskov, A. A. Velichko, A. L. Pergament, G. B. Stefanovich, and D. G. Stefanovich, “The effect of electric field on metal-insulator phase transition in vanadium dioxide,” *Tech. Phys. Lett.*, vol. 28, no. 5, pp. 406–408, May 2002.

- [18] S. Datta, N. Shukla, M. Cotter, A. Parihar, and A. Raychowdhury, “Neuro Inspired Computing with Coupled Relaxation Oscillators,” in *Proceedings of the The 51st Annual Design Automation Conference on Design Automation Conference - DAC '14*, 2014, pp. 1–6.
- [19] A. Parihar, N. Shukla, S. Datta, and A. Raychowdhury, “Exploiting Synchronization Properties of Correlated Electron Devices in a Non-Boolean Computing Fabric for Template Matching,” *IEEE J. Emerg. Sel. Top. Circuits Syst.*, vol. 4, no. 4, pp. 450–459, Dec. 2014.
- [20] N. Shukla *et al.*, “Pairwise coupled hybrid vanadium dioxide-MOSFET (HVFET) oscillators for non-boolean associative computing,” in *2014 IEEE International Electron Devices Meeting*, 2014, p. 28.7.1-28.7.4.
- [21] A. Velichko, M. Belyaev, V. Putrolaynen, A. Pergament, and V. Perminov, “Switching dynamics of single and coupled VO₂ -based oscillators as elements of neural networks,” *Int. J. Mod. Phys. B*, vol. 31, no. 2, p. 1650261, Jan. 2017.
- [22] S. Ghosh, “Generation of high-frequency power oscillation by astable mode arcing with SCR switched inductor,” *IEEE J. Solid-State Circuits*, vol. 19, no. 2, pp. 269–271, Apr. 1984.
- [23] C. . Chen *et al.*, “Resonant-tunneling-diode relaxation oscillator,” *Solid. State. Electron.*, vol. 44, no. 10, pp. 1853–1856, Oct. 2000.
- [24] A. A. Sharma, J. A. Bain, and J. A. Weldon, “Phase Coupling and Control of Oxide-Based Oscillators for Neuromorphic Computing,” *IEEE J. Explor. Solid-State Comput. Devices Circuits*, vol. 1, pp. 58–66, Dec. 2015.
- [25] N. Locatelli, V. Cros, and J. Grollier, “Spin-torque building blocks,” *Nat. Mater.*, vol. 13, no. 1, pp. 11–20, Jan. 2014.
- [26] A. A. Velichko, G. B. Stefanovich, A. L. Pergament, and P. P. Boriskov, “Deterministic noise in vanadium dioxide based structures,” *Tech. Phys. Lett.*, vol. 29, no. 5, pp. 435–437, May 2003.
- [27] A. Velichko, M. Belyaev, V. Putrolaynen, V. Perminov, and A. Pergament, “Modeling of thermal coupling in VO₂-based oscillatory neural networks,” *Solid. State. Electron.*, vol. 139, pp. 8–14, Jan. 2018.
- [28] A. Velichko, V. Putrolaynen, and M. Belyaev, “Effects of Higher Order and Long-Range Synchronizations for Classification and Computing in Oscillator-Based Spiking Neural Networks,” Apr. 2018.
- [29] M. Belyaev, A. Velichko, V. Putrolaynen, V. Perminov, and A. Pergament, “Electron beam modification of vanadium dioxide oscillators,” *Phys. status solidi*, vol. 14, no. 3–4, Dec. 2016.
- [30] A. Velichko, M. Belyaev, V. Putrolaynen, and P. Boriskov, “Method of increasing the information capacity of associative memory of oscillator neural networks using high-order synchronization effect,” May 2018.
- [31] M. Reljan-Delaney and J. Wall, “Solving the linearly inseparable XOR problem with spiking neural networks,” in *2017 Computing Conference*, 2017, pp. 701–705.